Numerical Study of Natural Convection from Discrete Heat Sources in a Vertical Square Enclosure

G. Refai Ahmed* and M. M. Yovanovich†
University of Waterloo, Waterloo, Ontario, N2L 3G1 Canada

A numerical finite difference technique based on the Marker and Cell **(MAC)** method is used to obtain solutions of a two-dimensional model of a square enclosure with laminar natural convection heat transfer from discrete heat sources. **A** discrete heat source is located in the center of one vertical side representing a high-power integrated circuit **(IC).** The conservation equations are solved using the primitive variables: velocity, pressure, and temperature. Computations are carried out for $Pr = 0.72$, $A = 1$ and $0 \leq Ra \leq 10^6$ (Rayleigh number is based on the length of the heat source S divided by the aspect ratio A). The ratio ε of the heat source size to the total height lies in the range $0.25 \leq \varepsilon \leq 1.0$. Verification of numerical results are obtained at $Ra = 0$ (conduction limit) with an analytical conduction solution, and the dependence of Nu and total resistance on Ra, ε, and boundary conditions are studied. Relationships between Nu and Ra based on different scale lengths are examined. In addition, a relationship between Nu and Ra, based on S/A, are correlated as $Nu = Nu\,(Ra, \varepsilon)$ and extrapolation equations are developed to cover the range of Ra from $0 \leq Ra < 10^9$.

Nomenclature

A	=	aspect ratio of cavity, H/L
C_p	=	specific heat at constant pressure, kJ/kg·K
% Diff.	=	$[(R_{t_{num}} - R_{t_{anal}})/R_{t_{anal}}] \times 100\%$
Gr	=	Grashof number, $S^3\beta g(T_h - T_c)/\nu^2 A^3$
Gr^*	=	isoflux Grashof number, $S^4\beta g q/\nu^2 k A^4$
g	=	gravitational acceleration, m/s^2
H	=	height of the cavity, m
h	=	coefficient of heat transfer, W/m^2·K
h_y	=	local coefficient of heat transfer, W/m^2·K
k	=	thermal conductivity, W/m·K
L	=	width of cavity, m
Nu	=	average Nusselt number, hS/kA
P_d	=	nondimensional dynamic pressure
Pr	=	Prandtl number, ν/α
p_d	=	dimensional dynamic pressure, N/m^2
Q	=	total heat flow rate, W
q	=	heat flux at discrete heat source, W/m^2
Ra	=	Rayleigh number, $S^3\beta g(T_h - T_c)/\alpha\nu A^3$
Ra^*	=	isoflux Rayleigh number, $S^4\beta g q/\alpha\nu k A^4$
R_c	=	nondimensional constriction resistance
R_m	=	nondimensional material resistance
R_t	=	nondimensional total resistance
r_t	=	dimensional total resistance, WW
S	=	length of discrete heat source, m
T	=	temperature, K
t	=	time, s
U	=	nondimensional velocity component in X direction
u	=	dimensional velocity component in x direction, m/s
V	=	nondimensional velocity component in Y direction
v	=	dimensional velocity component in y direction, m/s
X	=	nondimensional coordinate
x	=	dimensional coordinate, m
Y	=	nondimensional coordinate
Y_1	=	nondimensional length, $[A(H - S)/2S]$
Y_2	=	nondimensional length, $[A(H + S)/2S]$
Y_3	=	nondimensional length, $[HA/S]$
y	=	dimensional coordinate, m
α	=	thermal diffusivity, $k/C_p\rho$, m^2/s
β	=	coefficient of thermal expansion, 1/K
ε	=	relative discrete heat source size, S/H
λ_n	=	eigenvalues defined in Eq. (6)
ν	=	kinematic viscosity, m^2/s
ρ	=	density, kg/m^3
τ	=	nondimensional time
Θ	=	nondimensional temperature, $T - T_c/T_h - T_c$ or $(T - T_c)kA/qS$
θ	=	temperature excess, $T - T_c$, K
$\tilde{\theta}_S$	=	area-average source temperature excess, $T_S - T_c$, K

Subscripts

anal	=	analytical solution
c	=	cold temperature
H	=	height of the cavity
h	=	hot temperature
L	=	width of the cavity
num	=	numerical solution
S	=	discrete heat source

Abbreviations

GE	=	governing equation
IFDHS	=	isoflux discrete heat source
ITDHS	=	isothermal discrete heat source
MAC	=	Marker and Cell

Mathematical Expressions

$$\frac{D}{Dt} = \frac{\partial}{\partial} + U\frac{\partial}{\partial X} + V\frac{\partial}{\partial Y}$$

Presented as Paper 90-0256 at the AIAA 28th Aerospace Sciences Meeting, Reno, NV, Jan. 8–11, 1990; received March 5, 1990; revision received Sept. 20,1990; accepted for publication Sept. 21,1990.

*Graduate Research Assistant, Microelectronics Heat Transfer Laboratory, Department of Mechanical Engineering. Member AIAA.
†Professor of Mechanical Engineering and Electrical Engineering, Microelectronics Heat Transfer Laboratory, Department of Mechanical Engineering. Associate Fellow AIAA.

Introduction

OVER the past twenty years, a revolution in electronics has taken place. The miniaturization which resulted from Large Scale Integration (LSI) of components has led to the microminiaturization of Very Large Scale Integration (VLSI). As a consequence of packing a very large number of components into one very small chip, the attendant volumetric heat generation rate has risen to extremely high levels. "The power per unit volume that must be dissipated by modern electronic devices is of the same order of magnitude as that of a pressurized water nuclear reactor" as noted by Kelleher.[1]

Natural convection cooling of components attached to printed circuit boards which are placed vertically in an enclosure is currently of great interest to the microelectronics industry. Natural convection cooling is desirable because it does not require an energy source, such as a forced air fan, and it is maintenance free and safe.

The enclosure, as shown in Fig. 1, consists of two vertical boundaries of height H, and two horizontal boundaries of length L. One vertical boundary is cooled at T_c and the other has a discrete heat source (isoflux q or isothermal T_h) on an otherwise adiabatic surface. The top and bottom horizontal boundaries are adiabatic.

The work of Chu and Churchill' represents a first contribution to the study of natural convection in an enclosure with concentrated heat sources. In this study a finite difference formulation using a two-dimensional mesh (10 x 10) was employed to solve the transient equations in order to obtain the steady state solution. The solutions presented in Reference 2 are for aspect ratios, $A = HIL$ of 0.4 to 5, Grashof number (based on the height of the cavity) from 0 to 10^5, and a Prandtl number of air. The size and location of the heater strip were also varied. More recently Turner and Flack[3] and Flack and Turner[4] conducted experiments in air and they confirmed the $A = HIL$ and $\varepsilon = S/H$ trends observed by Chu and Churchill,' but only for Grashof numbers ($5 \times 10^6 \leq Gr_H \leq 9 \times 10^6$). Keyhani et al.,[5,6] studied multiple discrete heat sources mounted vertically on cavity walls, for Rayleigh numbers (based on cavity width) $2000 \leq Ra_L^* \leq 10^8$.

From the above studies one finds that:

1) Different length scales were used in the definitions of the Nusselt number and the Rayleigh number (see Table 1). The choice of the characteristic length, as shown in the study of Chu and Churchill,' is arbitrary, but affects the results of Nusselt numbers or Rayleigh numbers significantly.

2) It is difficult to extend the numerical results to high Ra; but in this study an extrapolated correlation is given for Ra > 105.

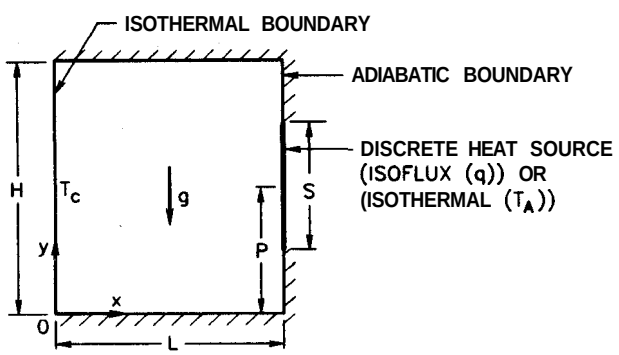

Fig. 1 Schematic of the enclosure.

Table 1 Scale lengths of *Nu*, *Ra* in previous studies for $Ra = 0$

Ref.	Scale length of *Nu*	Scale length of *Ra*
2	S	H
3, 4	H	H
5, 6	L	L

In the present study numerical results will be given for relative source lengths, ε, of 1, 0.75, 0.5, and 0.25 over the range $0 \leq Ra \leq 10^6$. Two limiting cases of a discrete beat source are examined: an isoflux discrete heat source (IFDHS) and an isothermal discrete heat source (ITDHS).

The paper is organized as follows. In the following section, the governing equations (GE) are stated with proper assumptions. In the third section, the nondimensional form of the (GE) is discussed. The numerical solution for (GE) is presented in the fourth section. The numerical results are discussed in the fifth section in the context of the flow regimes. The obtained and correlated results are discussed in the sixth section. Finally, conclusions are given in the last section.

Governing Equations and Conduction Solutions

Assumptions used in the present study are:

1) Fluid is considered as incompressible and Newtonian.
2) Flow is laminar in two dimensions x and y.
3) Thermal properties of the fluid are constant except in the buoyancy term "Boussinesq approximation."
4) Pressure changes inside the cavity are moderate.
5) Viscous dissipation effects are neglected.

For two-dimensional, laminar natural-convection inside enclosures, the governing equations of mass, momentum, and energy, can be written as follows:

$$\frac{\partial u}{\partial x} + \frac{\partial v}{\partial y} = 0 \tag{1}$$

$$\rho \frac{Du}{Dt} = -\frac{\partial p_d}{\partial x} + \mu \nabla^2 u \tag{2}$$

$$\rho \frac{Dv}{Dt} = \frac{\partial p_d}{\qquad} \quad \nabla^2 v - (\rho - \rho_0) g \tag{3}$$

$$\rho C_p \frac{DT}{Dt} = k \nabla^2 T \tag{4}$$

Analytical Solution for $Ra = 0$

A separable series solution to Laplace's equation $\nabla^2 T = 0$ can be used to solve the conduction problem. for Ra = 0, by taking $\theta = T - T_c$. The form of the solution, Eq. (5), satisfies the homogeneous condition at $x = 0$ and the adiabatic conditions along y = 0 and H

$$\theta(x, y) = a_0 x + \sum_{n=1}^{\infty} a_n \cos(\lambda_n y) \sinh(\lambda_n x) \tag{5}$$

or

$$\theta(x, \mathrm{y}) = \sum_{n=0}^{\infty} a_n \phi_n; \qquad \mathrm{A}, = n\pi/H \tag{6}$$

The temperature gradient is therefore

$$\frac{\mathrm{ae}}{\mathrm{ax}} = \sum_{n=0}^{\infty} a_n \phi_n' \tag{7}$$

The remaining boundary conditions along $x = L$ are

$$\frac{\mathrm{ae}}{\partial x} = 0 \quad 0 \leq y \leq \frac{H - S}{2} \qquad \frac{H + S}{2} \leq y \leq H \tag{8}$$

and for the IFDHS or ITDHS. we have

$$\frac{\partial v}{\partial x} = \frac{q}{k} \qquad \frac{H - S}{2} \leq y \leq \frac{H + S}{2} \tag{9}$$

or

$$\theta = \theta_h \qquad \frac{H - S}{2} \le y \le \frac{H + S}{2} \tag{10}$$

The Fourier coefficients a_n in Eq. (5) can be easily and accurately determined, for either the IFDHS or ITDHS, using a continuous variational approximation as noted in Lemczyk and Gladwell.[7] The overall enclosure resistance is defined by

$$r_t = \bar{\theta}_S/Q \tag{11}$$

For the IFDHS, the a_n in Eq. (5) are explicitly defined, since $\phi_n'(L, y)$ is continuous-along $0 \le y \le H$. Therefore, by using the area-averaging of $\bar{\theta}_S(\bar{\theta}_S = 1/S \int \theta_S dy)$ and dividing by Q, we can write

$$r_t = \frac{a_0 L}{qS} + \frac{1}{Sq\pi\varepsilon} \cdot \sum_{n=1}^{\infty} \frac{a_n[\sin(n\pi(1+\varepsilon)/2) - \sin(n\pi(1-\varepsilon)/2)]\sinh(n\pi/A)}{n} \tag{12}$$

a_0 and a_n are obtained by solving Eq. (6) at $x = L$ and $0 \le y \le H$ for IFDHS

$$a_0 = \frac{qS}{kH}$$

$$a_n = \frac{2qH}{k\pi^2} \sum_{n=1}^{\infty} \frac{[\sin(n\pi(1+\varepsilon)/2) - \sin(n\pi(1-\varepsilon)/2)]}{n^2\cosh(n\pi/A)}$$

Equation (12) will be as follows:

$$r_t = \frac{1}{A \cdot k \cdot 1} + \frac{2}{k \cdot \varepsilon^2 \cdot 1 \cdot \pi^3} \cdot \sum_{n=1}^{\infty} \frac{[\sin(n\pi(1+\varepsilon)/2) - \sin(n\pi(1-\varepsilon)/2)]^2\tanh(n\pi/A)}{n^3} \tag{13}$$

However, for the ITDHS, the a_n are not explicitly defined, but can be determined using the procedure developed in Reference 7. The solution was also checked against a conformal mapping solution[5] and found to agree within 1% for $0.25 \le \varepsilon \le 1$. In either case, however, the a_n are not explicit as in the IFDHS case. By nondimensionalizing Eq. (13), we obtain

$$R_t = 1.0 + \frac{A}{\pi^3\varepsilon^2} \sum_{m=1}^{\infty} \frac{\sin^2(m\pi\varepsilon)\tanh(2m\pi/A)}{m^3} \tag{14}$$

where $n = 2 \cdot m$.

From Eq. (14), one notes that the total resistance of the enclosure at $Ra = 0$ consists of the linear sum of the material and constriction resistances (R_m, R_c) where

$$R_t = \frac{\bar{\theta}_S kH}{qSL} = \Theta_S; \qquad \bar{\theta}_S = \bar{T}_S - T_c \tag{15}$$

The scale length S/A is naturally determined from Eq. (15). It has physical meaning because it depends on the heat source size and geometry of the enclosure.

Remark 1

The characteristic length S/A for an enclosure with a discrete heat source is obtained directly from the analytical solution of the governing equations when $Ra = 0$.

Nondimensional Form of the Governing Equations

The governing equations of mass, momentum, and energy Eqs. (1–4), can be written in nondimensional form as follows:

$$\frac{\partial U}{\partial X} + \frac{\partial V}{\partial Y} = 0 \tag{16}$$

$$\frac{DU}{D\tau} = -\frac{\partial P_d}{\partial X} + Pr\nabla^2 U \tag{17}$$

$$\frac{DV}{D\tau} = -\frac{\partial P_d}{\partial Y} + Pr\nabla^2 V + RaPr\Theta \tag{18}$$

$$\frac{D\Theta}{D\tau} = \nabla^2\Theta \tag{19}$$

with the nondimensional variables defined as

$$U = \frac{uS}{\alpha A} \qquad V = \frac{vS}{\alpha A} \qquad \tau = \frac{t\alpha A^2}{S^2}$$

$$X = \frac{xA}{S} \qquad Y = \frac{yA}{S} \qquad P_d = \frac{p_d \rho C_p^2 S^2}{k^2 A^2}$$

$$\Theta = \frac{T - T_c}{T_h - T_c} \quad \text{ITDHS}$$

$$\Theta = \frac{(T - T_c)kA}{qS} \quad \text{IFDHS}$$

The nondimensional initial and boundary conditions are given as

$$t = 0: \quad U = V = 0 \quad \Theta = 0$$

$$t \ge 0: \; X = \frac{LA}{S} \quad U = V = 0 \quad 0 \le Y \le Y_1 \quad \frac{\partial\Theta}{\partial X} = 0$$

$$Y_1 \le Y \le Y_2 \quad \frac{\partial\Theta}{\partial X} = -1 \quad \text{IFDHS}$$

$$Y_1 \le Y \le Y_2 \quad \Theta = 1 \quad \text{ITDHS}$$

$$Y_2 \le Y \le Y_3 \quad \frac{\partial\Theta}{\partial X} = 0$$

$$0 \le X \le \frac{LA}{S} \quad U = V = 0 \quad Y = 0 \text{ and } Y_3 \quad \frac{\partial\Theta}{\partial Y} = 0$$

The local and overall thermal energy balance at $x = L$ may be written as

$$h_y\theta_S = k\frac{\partial\theta}{\partial x} \tag{20}$$

and

$$h = \frac{1}{S\bar{\theta}_S} \int_{\frac{H-S}{2}}^{\frac{H+S}{2}} k\frac{\partial\theta}{\partial x}\, dy \tag{21}$$

The total heat flow rate at $x = L$, is given by

$$Q = q.S.1 = k.1 \int_{\frac{H-S}{2}}^{\frac{H+S}{2}} \frac{\partial\theta}{\partial x} dy = h.S.1\bar{\theta}_S \tag{22}$$

The area-average Nusselt number is defined as

$$Nu = \frac{qS}{kA\bar{\theta}_s} = \frac{1}{R_t} \tag{23}$$

Numerical Solution

A numerical solution of Eqs. (16–19) is sought subject to the conditions of no slip on all solid boundaries. Used in this study is a new version of a finite difference computer code, developed by Refai[9] based on the Marker and Cell (MAC) method, as carried out by Hirt et al.[10] The method uses a finite difference formulation with primitive variables as the dependent variables. The enclosure is, therefore, divided into a finite difference mesh of square cells (AX, ***AY***) surrounded by a single layer of fictitious cells where the boundary conditions are imposed as shown in Fig. 2. The fluid velocity components (U, V) are defined at each cell surface while the pressure and temperature (P_d, Θ) are located at the cell centers. Further details on this procedure can be found in Refs. (9) and (11).

Four steps were taken to validate the MAC technique used for the numerical solutions:

1) Test the convergence.

2) Compare the velocity and the temperature profiles for different ***Ra*** with previous studies.

3) Compare results with analytical solutions at $Ra = 0$.

4) Compare results of Nu with previous numerical and experimental studies.

Items 1 and 2 were carried out in detail by Refai[9] and Fath et al.[11] Tables 2 and 3 show the comparison between the analytical and numerical results when $Ra = 0$. The comparison between previous and present results will be discussed later.

Flow Regimes

Figure 3 shows the IFDHS case of nondimensional velocity profiles of the Y-component, V, at midheight of a vertical square enclosure for different Ra^*, $Pr = 0.72$ and ε. At $\varepsilon = 1$, as Ra^* increased from 10^3 (conduction regime) to 10^6 (laminar regime), the position of the maximum velocity moved closer to the vertical boundaries. Although the trends throughout the full flow regime are similar, the velocity profiles are slightly skewed towards the cold isothermal boundary. The nondimensional temperature distributions are shown in Fig. 4. For a discrete isoflux heat source, at $Ra^* = 10^3$, a linear distribution is obtained representing the conduction regime. For $Ra^* = 10^6$ (laminar regime), the distribution shows a slight negative temperature gradient in a portion of the enclosure as a result of the fluid motion. This has also been observed in previous numerical and experimental studies[11–13] but for full contact, $\varepsilon = 1$, and isothermal source.

The same trend for the velocity and temperature profiles is obtained for $\varepsilon = 0.25$ but at lower values of Ra^* as shown in Figs. 3b and 4b. This indicates that the change from conduction to laminar regime for the smallest ε occurs at lower Rayleigh numbers compared to $\varepsilon = 1$. For $\varepsilon = 0.25$ the Rayleigh numbers for conduction, transition from conduction, and laminar regimes are 3.9, 156, and 3906, respectively;

Table 2 Comparison between numerical and analytical solutions (IFDHS) at $Ra^* = 0$

ε		R_c	R_m	R_t	†% Diff.
0.25	*	0.354	0.999	1.353	1.05
	•	0.339	1.0	1.339	
0.50	*	0.141	0.999	1.141	0.44
	•	0.136	1.0	1.136	
0.75	*	0.039	0.999	1.039	0.1
	•	0.038	1.0	1.038	
1.0	*	0.0	0.999	0.999	−0.02
	•	0.0	1.0	1.0	

*Numerical results.
*Analytical results.
†% Diff. = $[(R_{num} - R_{anal})/R_{anal}] \times 100\%$

Table 3 Comparison between numerical and analytical solutions (ITDHS) at $Ra = 0$

ε		R_c	R_m	R_t	% Diff.
0.25	*	0.336	0.999	1.335	1.14
	•	0.32	1.0	1.32	
0.50	*	0.125	0.999	1.125	0.9
	•	0.115	1.0	1.115	
0.75	*	0.032	0.999	1.032	0.49
	•	0.0272	1.0	1.027	
1.0	*	0.0	0.999	0.999	−0.02
	•	0.0	1.0	1.0	

*Numerical results.
*Analytical results.

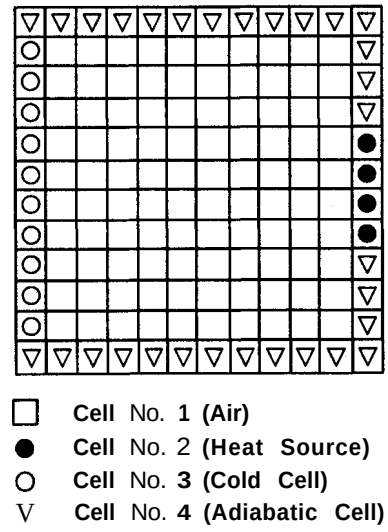

Fig. 2 Finite difference grid with flagged boundary cells: typical cell arrangement was 1 air cell; 2 to 4 boundary cells.

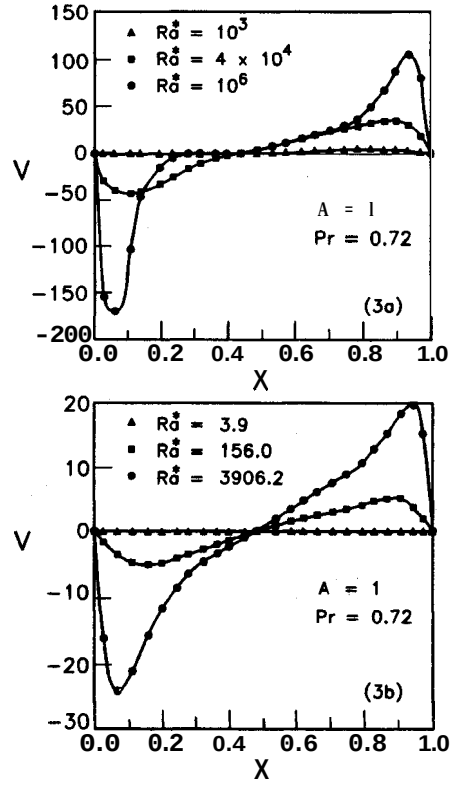

Fig. 3 Dimensionless velocity profiles at the midheight of the enclosure (IFDHS): a) $\varepsilon = 1$, b) $\varepsilon = 0.25$.

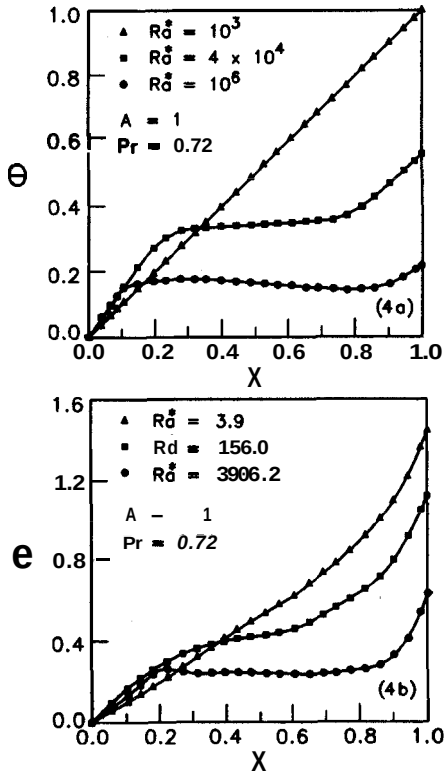

Fig. 4 Dimensionless temperature profiles at the Midheight of the enclosure (IFDHS) a) $\varepsilon = 1$, b) $\varepsilon = 0.25$.

however, for $\varepsilon = 1$ they are 1000, 4×10^4, and 10^6, respectively. On the other hand, the ratio between Rayleigh numbers in conduction and transition regimes for $\varepsilon = 0.25$ is 40, which is the same for $\varepsilon = 1$. The same observation for the ratio between conduction and laminar regimes is found for $\varepsilon = 0.25$, and 1; it is 10^3. The same observations were found for ITDHS.

Discussion of Results

Effect of Scale Length

The choice of scale length is very important because it alters the trend of the relationship between Nu and Ra. Figure 5a shows the relationship between Nu, and Ra_H^* using the height H or width L of the enclosure (square enclosure) as the scale length. By this definition, when ε decreases Nu, increases therefore $Nu, \rightarrow \infty$ at $\varepsilon \rightarrow 0$. On the other hand, Fig. 5b shows the relationship between Nu, and Ra_H^* for several values of the relative source size ε when Nu is based on the scale length S and Ra_H^* is based on the height of the cavity, as in Ref. *(2)*. These relationships cannot go to one asymptote, therefore it is difficult to correlate these relationships with one equation. In contrast, Fig. 6a shows the relationships between Nu and Ra^* when they are based on the scale length obtained from the analytical solution. At $Ra^* = 0$, it can be seen that if $\varepsilon < 1$, then $Nu < 1$, which clearly represents the conduction solution behavior. It is easily shown that the scale length used in the present study is exactly the length used in previous studies' [12–15] when the heat source completely covers the right vertical face.

Remark 2

For full contact heat source, $\varepsilon = 1$, the scale length of the present study is $SIA = L$ which is consistent with the previous studies.[9,12–15]

Heat Transfer Results

The results for a vertical enclosure using ITDHS or IFDHS are shown in Fig. 6a for different ε. It is found for Ra^* greater

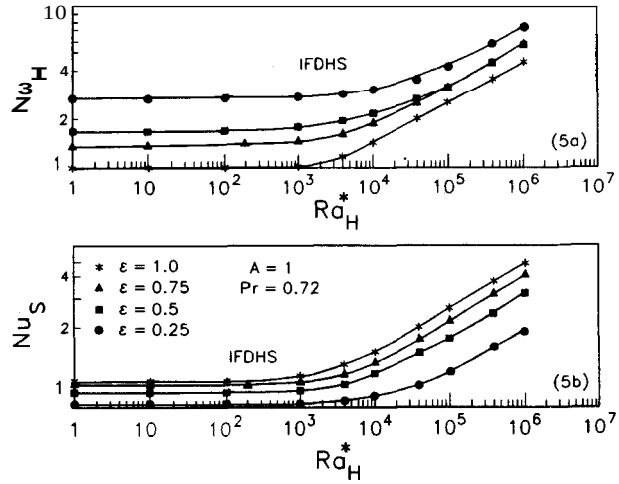

Fig. 5 *Nu-Ra* relationships for different scale lengths.

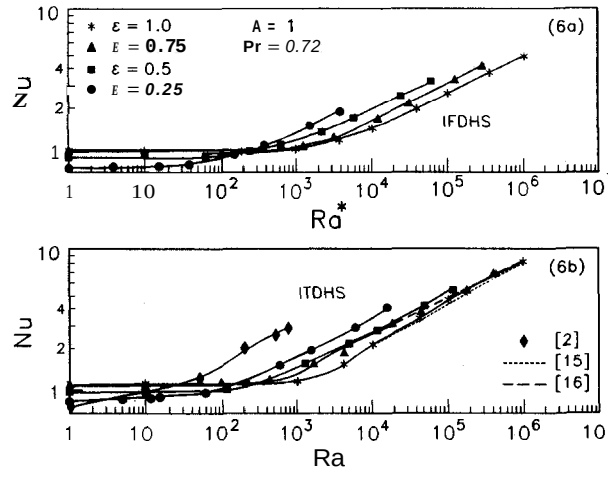

Fig. 6 *Nu-Ra* relationships depend on the scale length from the analytical solution.

than approximately 300 that Nu decreases with increasing ε, and the slope of log Nu vs log Ra^* is 0.26 at $\varepsilon = 1$ and 0.2 at $\varepsilon = 0.25$, for IFDHS. ITDHS follows the same trend as IFDHS but the slope of Ra is **0.3** at $\varepsilon = 1$ and 0.28 at $\varepsilon = 0.25$. Figure 6b shows good agreement between the present results and the experimental results of Eckert and Carlson[15] at $\varepsilon = 1$. The present results are closer to the experimental results[15] than the numerical results of Elder[16] also shown in Fig. 6b. The results of Chu and Churchill[2] show the same trend as the present results, if the scale length is changed to the recommended scale length.

Thermal Conductance and Thermal Resistance

To discuss both thermal resistance and thermal conductance, a question may be posed: Is it necessary to study this problem using new concepts? It is known that Nu is proportional to Ra; when $Ra \rightarrow \infty$, Nu will also go to infinity. Using the classical approach, it would have been difficult, if not impossible, to predict Nu beyond the range that is shown in Fig. **6.** By separating the effect of conduction from the Nusselt number, the change of thermal conductance can be obtained as defined by

$$Nu(Ra = 0) + \Delta Nu = Nu(Ra) \qquad (24)$$

where

$$Nu(Ra = 0) = 1/R_t \quad \text{and} \quad R_t = R_w + R_c$$

Utilizing the new approach, Fig. **7** shows that, for all ε, ΔNu increases with increasing Rayleigh. All curves of ΔNu

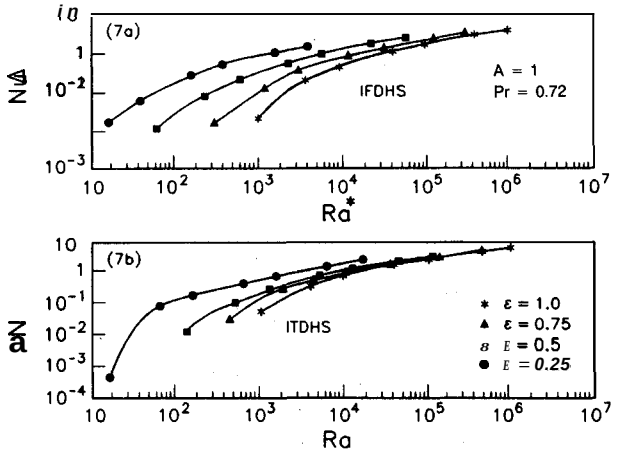

Fig. 7 ΔNu-Ra relationships.

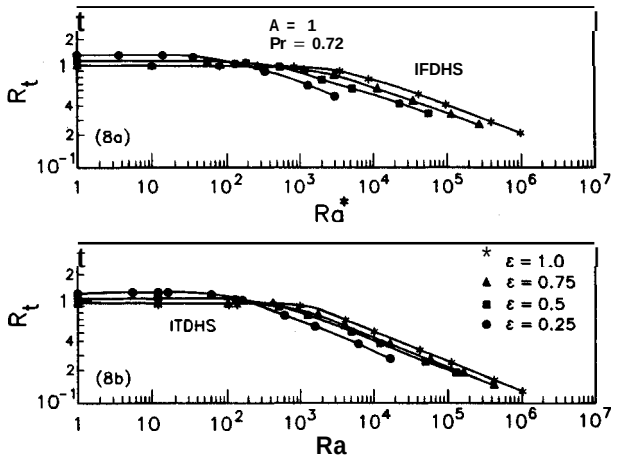

Fig. 8 R_t-Ra relationships.

approach a common asymptote tor both IFDHS and ITDHS, but the asymptotes of the two boundary conditions are slightly different. By estimating the slope of each asymptote, one can extend the relationship between ΔNu and Ra to include the higher end of Rayleigh ($Ra \to \infty$).

Remark 3

The scale length S/A also satisfies the following conditions:

1) It is defined by common parameters that do not change within the rectangular enclosure.

2) It is consistent with the physics of the problem.

3) It brings together natural convection results for various sizes of the heat source; therefore, it will be easy to obtain design correlations.

This concept is later used to extrapolate the correlation of Nusselt number as a function of Rayleigh. From Fig. 7 one observes that ΔNu is a function of ε, Ra_s, and the boundary conditions of the discrete heat source. However, at high Ra_s, ΔNu is not a function of ε. Nu ($Ra_s = 0$) will be very small compared to ΔNu, therefore, $Nu \simeq \Delta Nu$. On the other hand, Fig. 8 shows the relationship between the overall thermal resistance, R_s, and the Rayleigh number. One finds, when the Rayleigh number is smaller than approximately 300, R_s is independent of Ra_s, but it varies inversely with ε. In contrast, at Rayleigh numbers greater than 300, R_t strongly depends on Rayleigh number and it decreases with increasing Rayleigh number.

Remark 4

The relationship between Nu and Ra or Ra^* will approach a common asymptote line after separation of the effect of conduction from the overall Nusselt number.

Correlations of Nu-Ra Numerical Results

The complex dependence of Nu on Ra and ε apparently rules out obtaining a single equation that could correlate all results. Flack and Turner' obtained a separate correlation for each ε but it is difficult to use them as a design equation. The correlation for multidiscrete heat sources was obtained by Keyhani et al.,[5] but it is limited to their study only (i.e., $A = 4.5$). In the present study, correlations are obtained that include the effects of the boundary conditions and the relative size of the discrete heat source. The method suggested by Churchill and Usagi[17] was found to be remarkably successful in correlating rates of transfer for processes which vary uniformly between two asymptotes. A least-squares method was used to correlate the data for each asymptote as shown in Eqs. (25) and (27). In contrast, to develop Eqs. (26) and (28) for high Rayleigh numbers, we used Fig. 7 to estimate the slope of the relationship between ΔNu and Rayleigh. This relationship is a straight line on a log-log plot; then the effect of conduction at $Ra = 0$ was added to these correlations. The correlations are listed below.

1) IFDHS, $0 \le Ra^* \le 10^6\varepsilon^4$

$$Nu = [\varepsilon^{1.511} + (0.21\varepsilon^{-0.288}(Ra^*)^{0.221})^{17/2}]^{2/17} \quad (25)$$

For $10^5 \le Ra^*$

$$Nu = \varepsilon^{0.2} + 0.0302(Ra^*)^{0.35} \quad (26)$$

2) ITDHS, $0 \le Ra \le 10^6\varepsilon^3$

$$Nu = [\varepsilon^{1.7} + (0.146\varepsilon^{-0.256}Ra^{0.287})^{17/2}]^{2/17} \quad (27)$$

For $10^5 \le Ra$

$$Nu = \varepsilon^{0.2} + 0.0558Ra^{0.35} \quad (28)$$

The average difference between the numerical results and the correlations (25) and (27) is **4.3%**. The maximum difference of 8.7% occurs at the intersection of the two asymptotes. The comparison between the present high Rayleigh number correlations, Eqs. (26) and (29), and the experimental results of MacGregor and Emery[13] for $\varepsilon = 1$ and IFDHS is very good. The maximum absolute difference is 6.2% at $Ra^* = 10^8$. Table 4 shows this comparison in the range of Rayleigh number ($10^6 \le Ra^* \le 10^9$). Also the comparison between Eq. (28) and the correlation of the experimental study of Eckert and Carlson,[15] Eq. (30), is excellent; the maximum difference is 3% as shown in Table 5. The experimental results of MacGregor and Emery[13] are correlated by the following equation:

$$Nu = 0.046(Ra^*)^{.333} \quad (29)$$

Table 4 Comparison between the present study and MacGregor and Emergy[13] at A = 1 and $\varepsilon = 1$

Ra^*	Eq. (26)	Eq. (29) by [13]	% Diff.
10^6	4.8	4.6	4.3
10^7	9.5	9.9	−3.9
10^8	20.1	21.4	−6.2
10^9	43.7	46	−5.1

Table 5 Comparison between the present study and Eckert and Carlson[15] at A = I and $\varepsilon = 1$

Ra	Eq. (28)	Eq. (30) by [15]	% Diff.
10^5	4.14	4.15	−0.3
10^6	8.02	8.25	−3.1
10^7	16.7	16.5	1.3

The isothermal data of Eckert and Carlson[15] for $\varepsilon = 1$ and $1 \leq A \leq 20$ are correlated by

$$Nu = 0.131 Ra^{0.3} A^{-0.1} \tag{30}$$

From the good agreement between the previous experimental studies and Eqs. (26) and (28), one can expect good results for ε less than one.

Conclusions

These are the initial results from an ongoing research program into natural convection heat transfer from discrete heat sources in an enclosure.

The effect of a discrete heat source on natural convection heat transfer inside a square enclosure has been studied for different boundary conditions: ITDHS or IFDHS.

By studying this problem as a conduction problem when $Ra = 0$, the scale length S/A was obtained. It is also important to consider the effect of the thermal resistance and change of thermal conductance ΔNu. Correlations of Nu at high Ra appear to depend on the effect of change of thermal conductance ΔNu. Good agreement between the present results and the experimental results of MacGregor and Emery[13] and Eckert and Carlson[15] was obtained.

Correlation equations were developed for $0.25 \leq \varepsilon \leq 1$ and $0 \leq Ra < 10^9$.

Acknowledgments

The authors wish to acknowledge the financial support of the Natural Sciences and Engineering Research Council of Canada under Grant No. A7455. The authors also thank T. F. Lemczyk and J. R. Culham of the Microelectronics Heat Transfer Laboratory for their help.

References

'Kelleher, D. M., "Foreword," ***Heat Transfer in Electronic Equipment,*** HTD-Vol. 20, ***ASME Winter Annual Meeting,*** Washington, DC, 1981, pp. iii.

[2]Chu, H. H., and Churchill, S. W., "The Effect of Aspect Ratio and Boundary Conditions on Two-Dimensional Laminar Natural Convection in Rectangular Channels," ***ASME Journal of Heat Transfer,*** Vol. 98, No. 2, 1976, pp. 194–201.

[3]Turner, B. L., and Flack, R. D., "The Experimental Measurement of Natural Convection Heat Transfer in Rectangular Enclosures with Concentrated Energy Sources," ***ASME Journal of Heat Transfer,*** Vol. 102, No. 2, 1980, pp. 236–241.

[4]Flack, R. D., and Turner, B. L., "Heat Transfer Correlations for Use in Naturally Cooled Enclosures with High-Power Integrated Circuits," ***IEEE Transactions on Components, Hybrids and Manufacturing Technology,*** Vol. CHMT-3, 1980, pp. 449–452.

[5]Keyhani, M., Prasad, V., and Cox, R., "Natural Convection in a Vertical Cavity with Discrete Heat Sources," ***ASME Journal of Heat Transfer,*** Vol. 110, No. 3, 1988, pp. 616–624.

[6]Keyhani, M., Prasad, V., Shen, R., and Wong, T. T., "Free Convection Heat Transfer from Discrete Heat Sources in Vertical Cavity," HTD-Vol. 100, ***The Winter Annual Meeting of ASME,*** Chicago, IL, 1988, pp. 13–24.

[7]Lemczyk, T. F., and Gladwell, G. M. L., Personal Communication, University of Waterloo, Ontario, Canada.

[8]Schneider, G. E., and Yovanovich, M. M., "Thermal Resistance of Two-Dimensional Geometries Having Isothermal and Adiabatic Boundaries," ***Heat Transfer and Thermal Control,*** edited by A. L. Crosbie, Vol. 28, Progress in Astronautics and Aeronautics, AIAA, New York, 1981.

[9]Refai, G., "Numerical Study of Natural Convection Heat Transfer in Vertical and Inclined Enclosed Fluid Layers," Master's Thesis, Department of Mechanical Engineering, University of Alexandria, Alexandria, Egypt.

[10]Hirt, C. W., Nichols, B. D., and Romero, N. C., "Sola-A Numerical Solution Algorithm for Transient Flows," Report No. LA-5852, Los Alamos Labs., Los Alamos, NM, 1975.

[11]Fath, H. E. S., ElSherbiny, S. M., and Refai, G., "Influence of Prandtl Number and Boundary Condition on Heat Transfer in Vertical and Inclined Fluid Layers," HTD-Vol. 99, ***ASME Winter Annual Meeting,*** Chicago, IL, 1988, pp. 17–22.

[12]Chan, A. M., and Banerjee, S., "Three Dimensional Numerical Analysis of Transient Natural Convection in Rectangular Enclosures," ***Journal of Heat Transfer,*** Vol. 101, 1979, pp. 114–119.

[13]MacGregor, R. K., and Emery, A. F., "Free Convection Through Vertical Plane Layers-Moderate and High Prandtl Number Fluids," ***Journal of Heat Transfer,*** Vol. 91, 1969, pp. 391–403.

[14]ElSherbiny, S. M., Raithby, G. D., and Hollands, K. G. T., "Heat Transfer by Convection in Vertical and Inclined Air Layers," ***Journal of Heat Transfer,*** Vol. 104, No. 1, 1982, pp. 96–102.

[15]Eckert, E. R. G., and Carlson, W. D., "Natural Convection in an Air Layer Enclosed Between Two Vertical Plates with Different Temperatures," ***International Journal of Heat and Mass Transfer,*** Vol. 2, 1961, pp. 106–120.

[16]Elder, J. W., "Numerical Experiments with Free Convection in a Vertical Slot," ***Journal of Fluid Mechanics,*** Vol. 92, 1966, pp. 823–843.

"Churchill, S. W., and Usagi, R., "A General Expression for the Correlation of Rates of Transfer and other Phenomena," ***Journal of AICHE,*** Vol. 18, No. 6, pp. 1121–1128.